JOURNAL OF GEOPHYSICAL RESEARCH, VOL. 105, NO. E3, PAGES 6983–6995, MARCH 25, 2000

Geologic evolution of southern Rusalka Planitia, Venus

Heather R. DeShon,[1] Duncan A. Young, and Vicki L. Hansen

Department of Geological Sciences, Southern Methodist University, Dallas, Texas

Abstract. Geologic mapping of southern Rusalka Planitia, Venus, reveals interactions of volcanism, tectonism, and topography. We recognize three regional plains units (prR1, prR2, and prR3) based on crosscutting structural relations, embayment patterns, radar brightness, and surface roughness data. Delineation of secondary (tectonic) structures allows us to constrain the relative temporal relations between the three material units. Unit prR1, a radar dark smooth unit exposed in local topographic highs, hosts NE trending extension fractures. Low-viscosity lava flows of prR2, the most areally extensive unit, fill local topographic lows and the NE trending fractures. A shield-sourced lava unit, prR3, overlies prR2 on the basis of embayment relations and radar brightness. NW trending wrinkle ridges deform all three plains units and record regional contraction. Locally, flood lava flows that fill NE trending fractures are structurally inverted to form short, stepped NE trending wrinkle ridges. Map patterns indicate that prR2 comprises a thin layer (<50 m thick), much thinner than previous estimates of 1-3 km. Therefore previously proposed estimates of plains flood lava flow volumes and effusion rates are much too high. The local geologic history of southern Rusalka Planitia is inconsistent with global stratigraphy models. Our study supports the view of plains evolution occurring through discrete volcanic processes working at local and regional (but not global) scales.

1. Introduction

Plains, the most areally extensive geologic province on Venus, comprise over 80% of the planet's surface. Plains, variably defined in terms of hypsometry and radar character, reflect volcanic and tectonic geologic histories. Plains regions were first recognized and defined from Pioneer Venus altimetry data as flat low-lying areas generally below 1.5 km mean planetary radius (MPR, 6051.4 km) [*Masursky et al.*, 1980; *Ford and Pettengill*, 1992; *Banerdt et al.*, 1997]. Most plains regions lie between 6051.0 and 6052.8 km resulting in a unimodal hypsometric signature [*Rosenblatt et al.*, 1994]. On Magellan synthetic aperture radar (SAR) images, plains appear relatively radar dark, and hence smooth, compared to highland regions. This smoothness is interpreted to be the result of flood lava flows [*Head et al.*, 1992]. Venus plains commonly exhibit evidence of multiple minor deformation events, although they record significantly less deformation than highly deformed tessera regions [*Banerdt et al.*, 1997].

The fundamentally distinct topographic, volcanic, and tectonic elements of plains regions may have formed diachronously. The hypsometric signature of regional plains basins appears relatively young based on correlations between gravity and topography [*Herrick and Phillips*, 1991; *Rosenblatt et al.*, 1994]. However, the volcanic and tectonic history of the plains remains unresolved and may vary spatially across the planet. Tectonic structures preserved in plains units may provide a surface record of ancient climatic conditions and climate change [*Phillips and Hansen*, 1998; *Phillips and Bullock*, 1999; *Solomon et al.*, 1999; *Anderson and Smerkar*, 1999]. Understanding the geologic history of Venus' plains regions will lend valuable insight into crustal processes and the tectonic evolution of the planet.

Current debate over plains evolution concerns the temporal relations of material units and structures: Was plains evolution globally synchronous [e.g *Basilevsky et al.*, 1997; *Basilevsky and Head*, 1998; *Head and Basilevsky*, 1998] or localized in time and space [e.g *Phillips and Hansen*, 1998; *Guest and Stofan*, 1999]? In the global stratigraphic model the plains regions are divided into material units based on proposed global unconformities, suggesting that plains evolve through a globally synchronous sequence of geologic events [*Basilevsky et al.*, 1997; *Basilevsky and Head*, 1998; *Head and Basilevsky*, 1998]. *Basilevsky et al.* [1997] suggested that alternating globally extensive volcanism and deformation events resurfaced the planet ~300-500 m.y. ago, sculpting the vast plains preserved today. In this model, deformation events mark periods of global contraction or extension. Estimated lava flow volumes and effusion rates during this period of extensive plains formation are reported as the highest effusion rates in our solar system [*Head and Coffin*, 1997; *Solomon et al.*, 1999], requiring Venus volcanism to be unlike other known terrestrial processes. In contrast, *Guest and Stofan* [1999] and *Phillips and Hansen* [1998] proposed that plains volcanism and deformation occurred locally in space and time at effusion rates similar to terrestrial processes. *Guest and Stofan* [1999] proposed that the exposed plains regions form by a variety of eruptive and deformation styles that evolved spatially and temporally independent of one another. *Phillips and Hansen* [1998] proposed that plains volcanism (and tectonism) occurred throughout Venus history but that the rate of plains volcanism decreased over time as the Venusian lithosphere thickened globally. Even the highest proposed eruption rates in the

[1]Now at Department of Earth Sciences, University of California, Santa Cruz.

Paper number 1999JE001155.
0148-0227/00/1999JE001155$09.00

Phillips and Hansen [1998] model are similar to, or less than, those of terrestrial large igneous provinces.

We examine the geology of regional plains in southern Rusalka Planitia (~15°N-12°S, 150°-180°E) in order to determine local geologic history. Rusalka Planitia serves as the type location of Rusalka Group plains units in the global stratigraphy model [*Basilevsky and Head*, 1998; *Head and Basilevsky*, 1998]. Hence the geologic history of southern Rusalka Planitia provides constraints for models of global versus local plains formation. Our documented geologic history, as interpreted through detailed geologic mapping, records distinct periods of volcanism, tectonism (fracturing and folding), and topographic evolution. The interaction of these three components through time and space is inconsistent with the global stratigraphic model. Geologic relations between plains units indicate that some volcanic plains units are significantly thinner than previous estimates [*Basilevsky et al.*, 1997; *Kreslavsky and Head,* 1999; *Collins et al.*, 1999] and draw into question proposed high effusion rates [e.g *Head and Coffin*, 1997].

2. Background

Venus has been shaped by a variety of tectonic and volcanic processes imposed on a lithosphere stationary with respect to the mantle. Morphologically crustal plateaus, volcanic rises, coronae, rift or fracture zones, and plains regions mark Venus' surface. Temporally and spatially, most deformation is concentrated within high standing, 1000-2500 km diameter quasi-circular crustal plateaus supported by thickened crust. Although controversial, a growing body of evidence indicates that crustal plateaus and their characteristic structural fabric, known as tesserae, represent the surface signature of hot mantle plumes on ancient thin lithosphere [*Phillips and Hansen*, 1998; *Hansen et al.,* 1999]. Volcanic rises, regional-scale topographic domes that host rifts and shield volcanoes, represent the surface signature of mantle plumes on contemporary, relatively thick lithosphere [*Smrekar et al.,* 1997; *Phillips and Hansen*, 1998]. Coronae are large (generally 100-900 km diameter), quasi-circular volcanic ring structures probably related to mantle diapirism [*Stofan et al.,* 1997] and are commonly spatially associated with chasmata (deep troughs) and fracture zones. Plains regions, the focus of this paper, have predominantly been shaped by volcanic processes, although ridge belts, wrinkle ridges, fractures, and meteoroid impact craters variably deform the material units that comprise the plains. Geochemical analyses taken by the Vega landers within Rusalka Planitia indicate tholeitic basalt compositions, and although compositional details remain unresolved, these results have been interpolated to all Venusian plains [*Basilevsky et al.*, 1992; *Grimm and Hess*, 1997].

Regional plains display a variety of volcanic features and tectonic structures and forms of basaltic flood volcanism [*Guest et al.*, 1992; *Banerdt et al.*, 1997; *Basilevsky and Head*, 1998]. Typical plains volcanic features include extensive smooth flood lava flows, sinuous rilles, canali, and shield fields [*Crumpler et al.*, 1997]; tectonic structures include suites of fractures, wrinkle ridges, faults, and ridge belts [*McGill*, 1993; *Banerdt et al.*, 1997]. Flow fronts of plains units degrade over time because of chemical weathering [*Arvidson et al.,* 1992] making it difficult to determine unique contact relations and relative temporal relations between plains units. Proposed lava flow unit thickness, volume estimates, and effusion rates [*Basilevsky and Head*, 1996, 1998; *Head and Coffin*, 1998] are poorly constrained by currently available data. Although the term "plains" has been used to describe any radar dark, smooth, flooded feature on Venus [*Ivanov and Head*, 1996], we restrict our use to refer to spatially extensive radar dark (hence smooth) relatively flat, low-lying regions. We do not use the term plains in reference to local regions of relatively radar dark (hence smooth) features within tessera terrain.

Basilevsky and Head [1995, 1998] and *Basilevsky et al.* [1997] divided Venus' geologic history into five global phases that define their global stratigraphic model, from oldest to youngest: (1) global or semi-global tessera formation through intensive tectonic deformation dominated by early crustal shortening and late stage extension, (2) global plains formation through extensive basaltic volcanism, (3) global wrinkle ridge formation, (4) local plains volcanism, and (5) local rift, volcanic rise, and coronae chain formation. The globally extensive plains materials, the Guinevere Supergroup, is divided into four subgroups: (1) the Sigrun Group, densely fractured plains (Pdf) outcropping as kipukas; (2) the Lavinia Group, fractured and ridged plains (Pfr) including ridge belts (RB) outcropping as elongated kipukas; (3) the Rusalka Group, shield plains (Psh) and plains with wrinkle ridges (Pwr) covering 70-75% of the surface; and (4) the Atla Group, lobate (Pl) and smooth plains (Ps) that lack wrinkle ridges associated with rift zones and coronae. Within the Rusalka Group, plains with wrinkle ridges (Pwr) are further divided, on the basis of radar brightness, into locally preserved subunits: Pwr_1, an older dark unit, and Pwr_2, a younger, relatively bright unit. Global wrinkle ridge formation marks an unconformity between Rusalka and Atla plains formation proposed to have spanned 40-70 m.y. Although wrinkle ridge formation is treated as a global tectonic event occurring over a geologically brief time [*Basilevsky*, 1996], wrinkle ridges are used as defining material characteristics of the Pwr_1 and Pwr_2 lava flow units. That is, wrinkle ridges, a suite of tectonic (secondary) structures, characterize proposed material unit definitions.

Building on the global stratigraphic model, *Head and Coffin* [1997] proposed that Venus' plains are large igneous provinces (LIPs) orders of magnitude more voluminous than LIPs found on Earth, Moon, and Mars. *Head and Coffin* [1997] used the prevalence of sinuous canali in Venusian plains units as qualitative evidence for exceptionally high lava effusion rates. These workers assumed that tessera underlies essentially all plains regions and that exposed tesserae within crustal plateaus reflects upwarping of the global layer. *Basilevsky and Head* [1996] estimated volcanic plains thickness to be equal to crustal plateau height (~1-3 km) in order to cover most preexisting tessera topography. Using impact crater densities, *Basilevsky and Head* [1998] proposed that Sigrunian, Lavinian, and Rusalkian plains formation spanned ~100 million years. *Head and Coffin* [1997] used the above thickness and temporal estimates to calculate plains volumes of ~9.2×10^8 km^3 and effusion rates of 5-7 km^3/yr. These estimates rely exclusively on geologic history assumptions inherent to the global stratigraphic model.

3. Southern Rusalka Planitia

Our work focuses on a 6000 km^2 region in southern Rusalka Planitia (Figure 1). Surrounding geologic and geographic features of Rusalka Planitia include Llorona Planitia to the

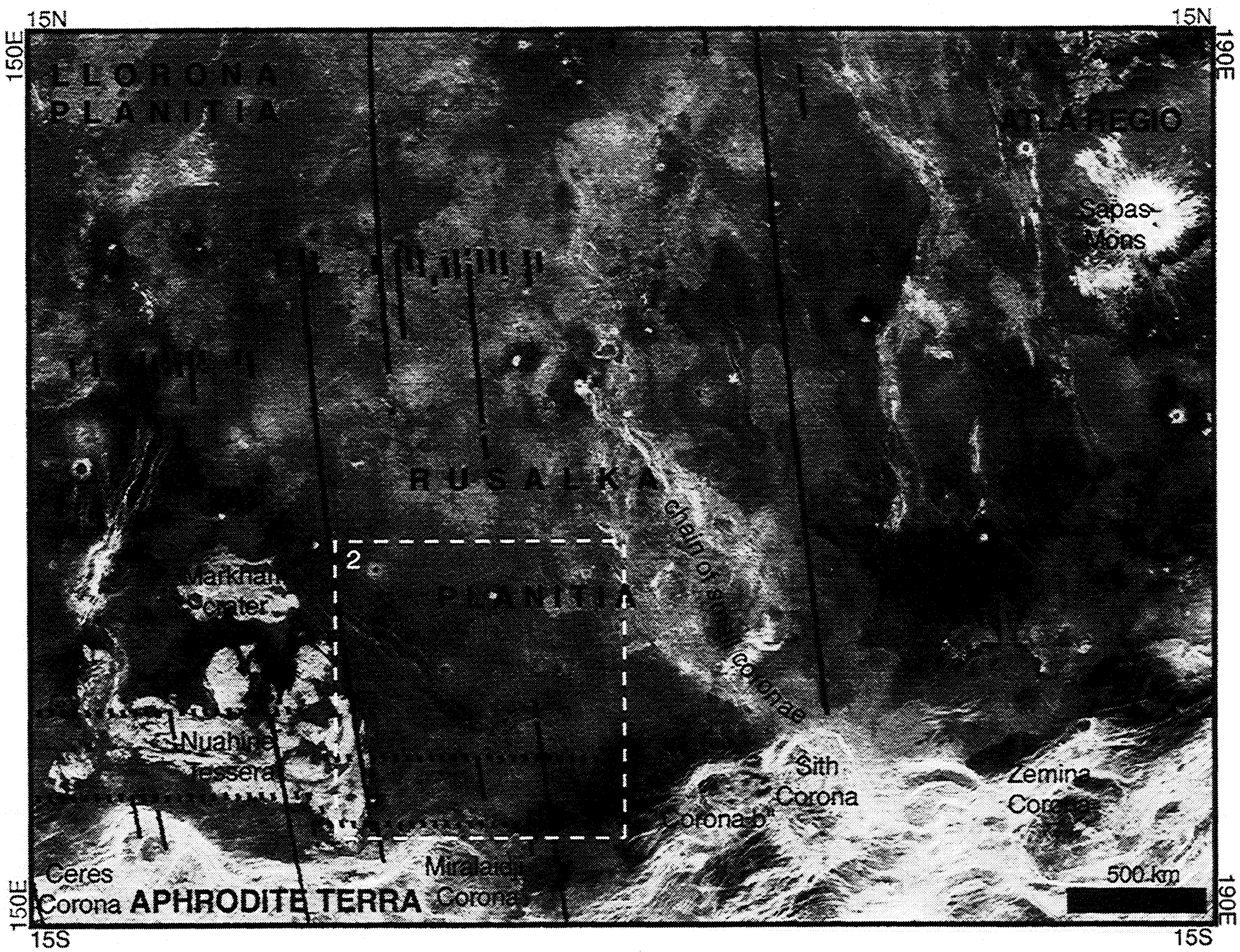

Figure 1. Synthetic aperture radar (SAR) image of Rusalka Planitia and surrounding geomorphic features. Image from C314N180;1. Box shows location of Figure 2.

north and the eastern Aphrodite Terra coronae chain and fracture zone to the south (Figure 1). Atla Regio, a volcanic rise that includes Sapas Mons, Maat Mons, and Ozza Mons, borders Rusalka Planitia to the east (Figure 1). Primary (emplacement related) structures in the planitia include small shields and canali (we use the term canali following *Baker et al.* [1992]). Secondary (tectonic) structures include a regional wrinkle ridge set that trends generally northwest [*Lancaster and Guest*, 1994; *Bilotti and Suppe*, 1999], various fractures and faults, and ridges and fractures associated with a chain of small coronae that extends northwest through the central region of the planitia. Southern Rusalka Planitia, a microcosm of the larger planitia, contains the tectonic features and orientation trends listed above (Figure 2).

We conducted detailed geologic and structural mapping of a 10° x 10° area in the southern part of Rusalka Planitia using Magellan SAR cycle 1, 2, and 3 full resolution (FMIDR) images and GxDR altimetry, emissivity, and slope data where available (Figures 1 and 2). Unit names and symbols used herein derive from geologic mapping in progress in the Diana Chasma Quadrangle (V37) [*DeShon and Hansen*, 1998; H. R. DeShon and V. L. Hansen, submitted manuscript, 1999] and follow U.S. Geological Survery/NASA VMAP program mapping guidelines [*Tanaka,* 1994]. The Interactive Data Language (IDL) program and Image SXM software allowed mosaicing of FMAP data and the adjustment of image properties for detailed mapping. Map information was compiled digitally. SAR data interpretation of geologic units and structures follows the methods for Magellan data analysis outlined by *Ford et al.* [1993].

3.1. Geologic Relations

Local geologic features include a tessera inlier, four plains units, three impact craters, and several coronae-related volcanic flows (Figures 2 and Plate 1). The Nuahine ridged tessera inlier (tNr) comprises possibly the oldest locally deformed crust. A 20-60 km wide swath of radar dark homogeneous plains unit surrounds the inlier along its south and east margins and appears continuous with intratessera volcanic material. The composite unit phc (homogeneous plains) consists of intratessera basin material and flood basalt lava flows likely related to regional plains formation; the unit is undivided owing to a lack of boundary constraints. Three regional plains units, differentiated by crosscutting relations, radar backscatter, and surface roughness data, comprise

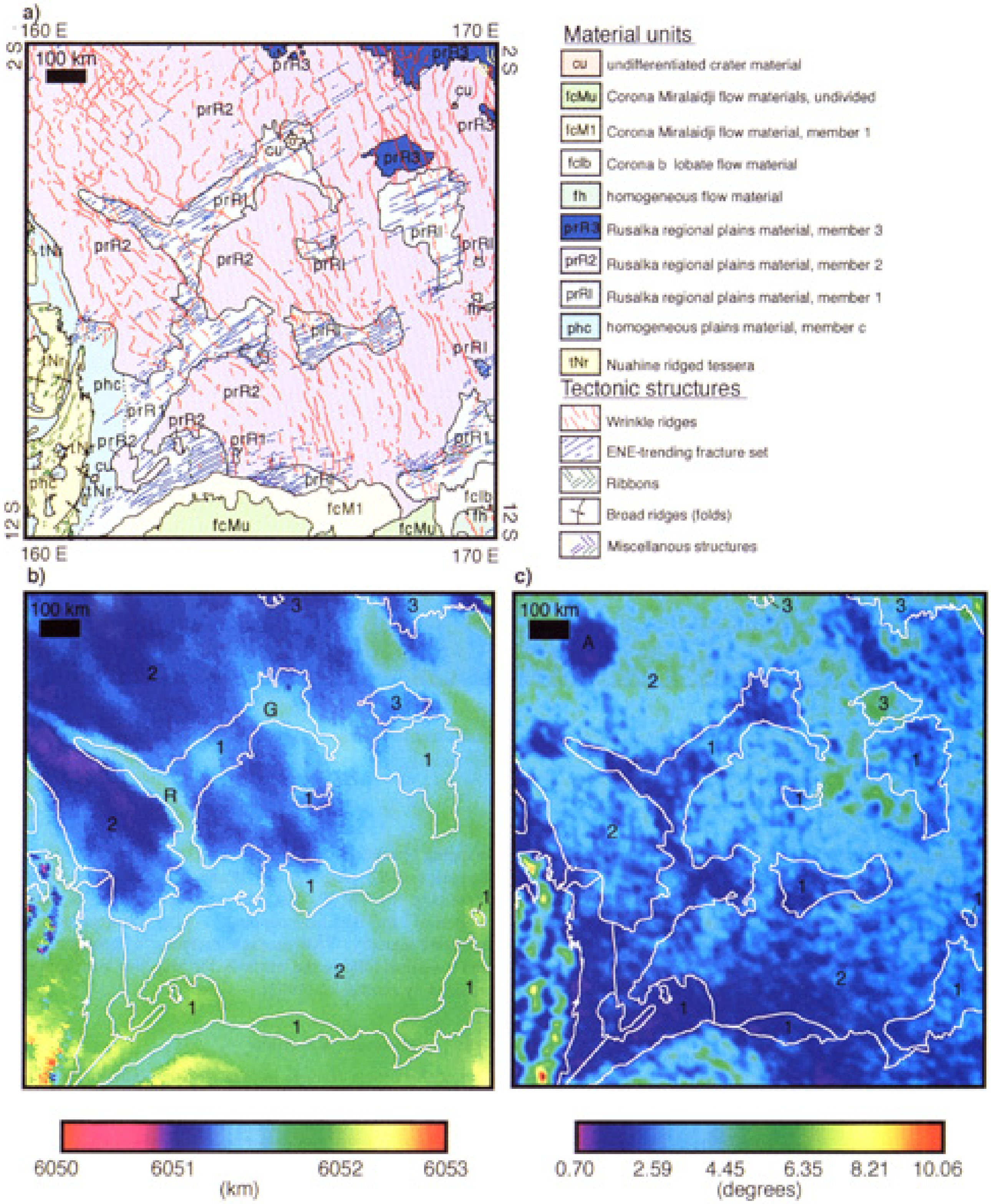

Plate 1. Southern Rusalka Planitia (a) geologic map, (b) altimetry (from GTDR 3;1), and (c) root mean squared surface roughness data (from GSDR 3;1). Labels in Plates1b and 1c include unit contacts, white lines (prR1 = 1, prR2 = 2, and prR3 = 3); airburst, A; ridge, R; gentle rise, G. Note temporal relationships between many units are unconstrained; see text for more complete discussion of relative timing.

Figure 2. Left-look SAR image of the southern Rusalka Planitia study area from fl06S162 FMAP (minor data gaps filled by right-look C200N183;201). Boxes show locations of Figures 4 and 5.

southern Rusalka Planitia: Rusalka regional plains materials, members 1, 2, and 3 (prR1, prR2, and prR3, respectively). Secondary (tectonic) structures that variably cut the plains units include suites of NE to ENE trending fractures and NW and locally developed NE-trending wrinkle ridges. A suite of concentric fractures related to Miralaidji Corona and fractures associated with coronae located outside the study area also cut the plains units. Coronae-associated volcanic flows related to both Miralaidji Corona (fcM1 and fcMu) and an unnamed corona (fclb) are relatively young units. Three impact craters and associated ejecta (cu, crater materials undivided) postdate local-host plains units but provide no other regional timing relationships. The diffuse pale spot in SAR (Figure 2) located at 3.5° S, 161.7° E is an impact airburst based on a low surface roughness anomaly and distinct radar characteristics.

Tessera terrain and coronae-related lava flows sit topographically higher than plains units (Plate 1b). Plains units ramp up to the coronae platform and hence are higher to the south. Broad topographic ridges trend NW with ~200-300 km spacing. The western most ridge (Plate 1b) is a class I ridge belt [*Kryuchkov*, 1988; *Banerdt et al.*, 1997] owing to its simple arch morphology. The arch, with up to 600 m of relief relative to local plains, is 170 km wide and extends ~900 km. An ~300 m deep depression along the western flank indicates net strike-perpendicular relief of ~900 m. A gentle rise extends to the northeast for ~400 km from the ridge's eastern flank.

3.1.1 Material units. Southern Rusalka Planitia consists of three regional plains units (Plate 1a). Rusalka regional plains, member 1 (prR1) is a relatively SAR dark, smooth unit compared to the other plains units and exhibits low backscatter (-17.63 to –18.36 dB at 43.5° incidence angle). Topographically, prR1 is exposed within broad highs (Plate 1b) and locally forms kipukas within the other plains units. A sinuous, 60 km long canali cuts prR1 near 10.5°S, 163.5°E and postdates prR1 emplacement (Figure 3c). A regional NE to ENE trending extension fracture set cuts prR1 and the canali.

Lava flows of member 2 (prR2), marked by dark to moderately bright radar return (-16.11 to -16.75 dB at 44.1° incidence angle), form the most areally extensive unit. Unit prR2 produces a mostly contiguous map pattern with local isolated flows (Plate 1 and Figure 3d). Fractures that cut prR1 disappear from view at some distance from the prR1-prR2 contact (Figure 2 and Plate 1a); prR2 lava flows locally fill and cover NE trending fractures that cut prR1 (Figure 3b). The irregular prR1-prR2 contact in the south follows broad, gentle topography (Plate 1b). These relations indicate that prR2 lava flows are low viscosity flood-like lava flows, and fracture formation and some topographic uplift predate prR2 emplacement.

Plains member 3 (prR3) exhibits relatively high radar backscatter (-13.10 to -13.88 dB at 45.1° incidence angle) and a mottled texture; it hosts abundant shield fields and generally lobate flow fronts. Shields, primary structures, are interpreted as part of this unit because the lava flows seem to emanate from the constructional edifices rather than flow around the shield edifices; within the study area, there is no evidence to suggest that prR3 shields are buried by younger radar dark lava flows. Topographically, prR3 cannot be distinguished from prR2 (Plate 1b). Unit prR3 either fills, and hence covers, NE trending fractures or lies above fracture-filling prR2.

The root mean squared (RMS) slope parameter, which quantifies the topographic undulation of a terrain at tens of centimeter to kilometer scales [*Ford and Pettengill*, 1992; *Plaut*, 1993], shows a distinct 1° increase between prR1 (which has a modal RMS slope of 2.3°, close to the planetary mode) and prR2 and prR3 (both of which have modal RMS slopes of ~3.3°) (Plate 1c). Tectonic terrains cut by numerous fractures yield RMS slope values as high as 10°, whereas the plains typically show ranges of 1°-3° [*Plaut,* 1993]. Therefore the NE trending fracture set may make prR1 appear rougher, suggesting that the average roughness of a theoretically non fractured prR1 may be lower than measured RMS values. SAR backscatter variations, determined by centimeter-scale surface roughness, also indicate a difference in unit roughness of prR1 and prR2. The backscatter for both surfaces, however, is consistent with lava flow surfaces of "moderate roughness" at the decimeter scale [*Arvidson et al.*, 1992; *Farr,* 1993]. Although prR2 and prR3 are generally indistinguishable in RMS data (Plate 1c), prR3 exhibits higher radar backscatter than prR2, indicating centimeter-scale textural differences between the two units.

3.1.2. Tectonic structures. NE trending fractures that cut prR1 help define stratigraphic and temporal relations between prR1 and the other southern Rusalka Planitia units (assuming that the fractures formed during a relatively distinct time interval). Lack of shear displacement along the fractures and consistent straight (i.e., non undulating) fracture boundaries indicate that the fractures are likely extension fractures [*Twiss and Moores*, 1992]. The NE trending fracture set consists of one to five radar bright lineaments per fracture. Fracture characteristics include spacing of ~3-10 km, lengths from 10 to >100 km, and widths that change from up to 1-1.5 km in the south to 0.1-1 km in the north. Wider fractures in the south have two to four terraces, or steps, as evidenced by more radar bright lineaments, defining each edge (Figure 3). These fractures have topographically raised edges, giving the fracture a distinctive double-lipped appearance. In the north, NE trending fractures thin and lose this wide, multiple-edged appearance. The consistent spacing and trend of all these fractures implies that these fractures represent a single, genetically related fracture set, even though fracture appearance changes perpendicular to the fracture trend across ~1000 km. We cannot uniquely determine, based on fracture spacing, if deformation occurred (1) in the upper layer of a single unit, (2) throughout an entire unit, or (3) in multiple units. Such limited constraints make any interpretations of the thickness of prR1 and possible underlying unit(s) nonunique.

The decrease in fracture width from south to north may indicate (1) a decrease in strain from south to north, (2) mechanical control related to underlying material anisotropy, or (3) differences in reactivation of NE trending fractures. These distinctive fractures may be the manifestation of the opening tensile fractures followed by local deflection and uplift of fracture edges due to contraction, resulting in multiple, topographically raised edges along the original fracture trend. The fractures may also record local thermal effects or increased strain related to corona formation. The deformation history of the multiple-edged fractures and the rheological characteristics of the host material remain unresolved.

Along the prR1-prR2 contact, NE trending fractures that cut prR2 appear relatively poorly defined and radar dark compared to the parallel fractures that cut prR1 (Figure 3). The NE trending fractures cease to affect prR2 ~100-300 km from the prR1-prR2 contact. Locally, prR2 flows along and within NE trending fractures resulting in a digitate contact between prR1 below and PrR2 above (Figure 3b). These relations indicate that prR2 covers the NE trending fractures by locally filling them with flow material; therefore prR2 emplacement postdates NE fracture formation.

NW trending wrinkle ridges spaced ~5-30 km deform prR1, prR2, and prR3. The dominant wrinkle ridge trend is part of a broadly circum-Aphrodite corona wrinkle ridge system described by *Bilotti and Suppe* [1999]. The wrinkle ridges parallel the trend of the class I ridge belt (Figure 2 and Plate 1b and 1c) discussed above, with wrinkle ridge spacing decreasing with proximity to the ridge belt. In the western half of the map area, short NE trending wrinkle ridges appear between ~7°S-2°S creating a polygonal wrinkle ridge pattern [*DeShon and Hansen*, 1998] (Figures 2, 4 and Plate 1). The polygonal pattern broadly correlates with both a geoid and a topography low (R. J. Phillips, personal communication, 1998). These correlated geoid/topography lows likely indicate local contraction and, possibly, ongoing topographic development.

NE trending wrinkle ridges are coincident with earlier formed and filled NE trending fractures (Figure 4). NE trending wrinkle ridges are straighter and shorter (5-10 km as opposed to 45-60 km) than NW trending wrinkle ridges. The

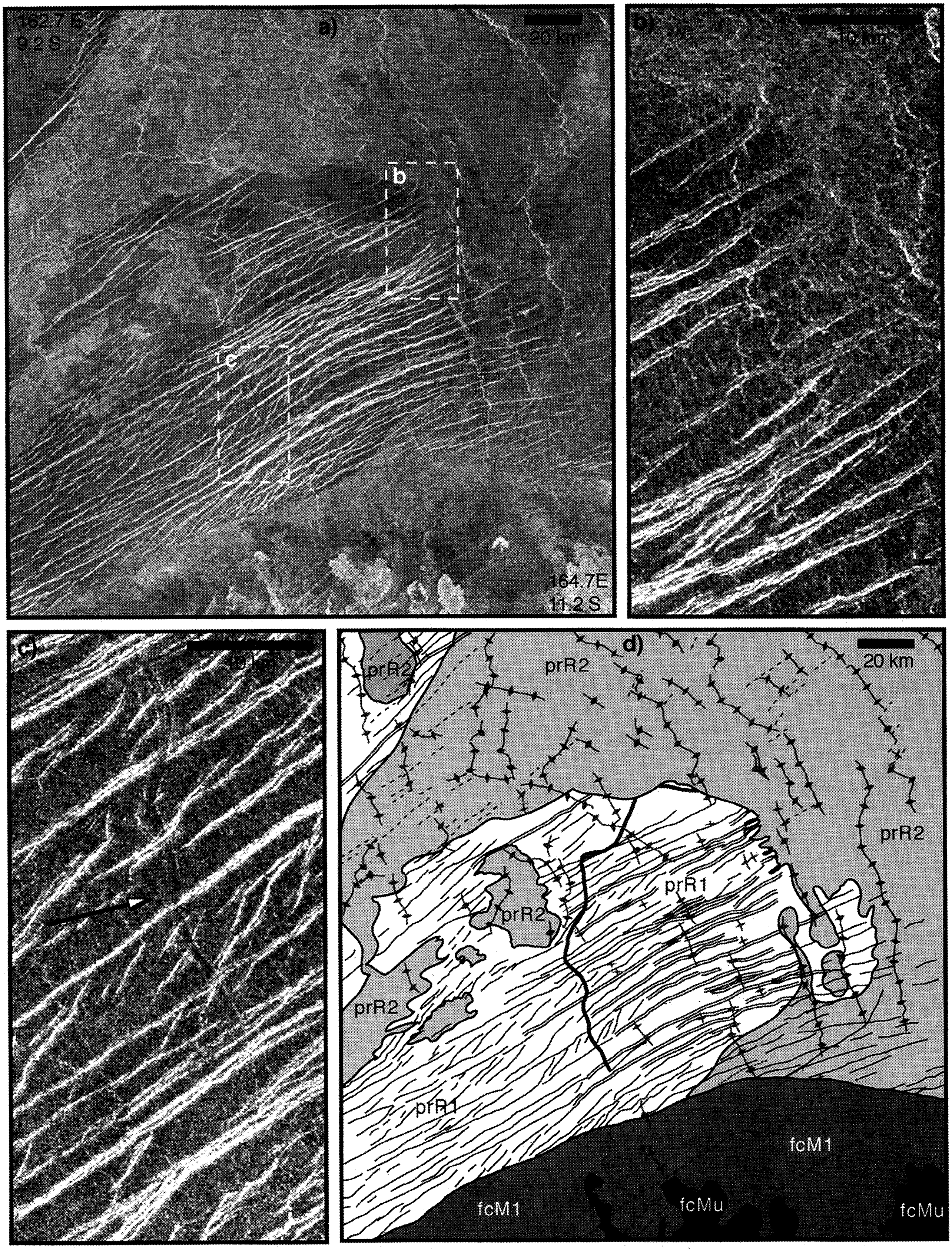

Figure 3. SAR and geologic map of NE trending fractures that cut unit prR1(location given in Figure 2). (a) 2°x2° SAR image tiled from left-look FMAP f106S162 (data gaps in top 30 km patched with right-look data); (b) detail of prR2 lava flows filling NE trending fractures that cut prR1; (c) detail of open fractures that postdate a canali, which in turn cuts (and therefore postdates) prR1 (arrow indicates illumination direction); (d) geological map of region shown in Figure 3a; structures include NE trending fractures (solid and double solid lines), canali (thick line), and wrinkle ridges (lines with diamonds).

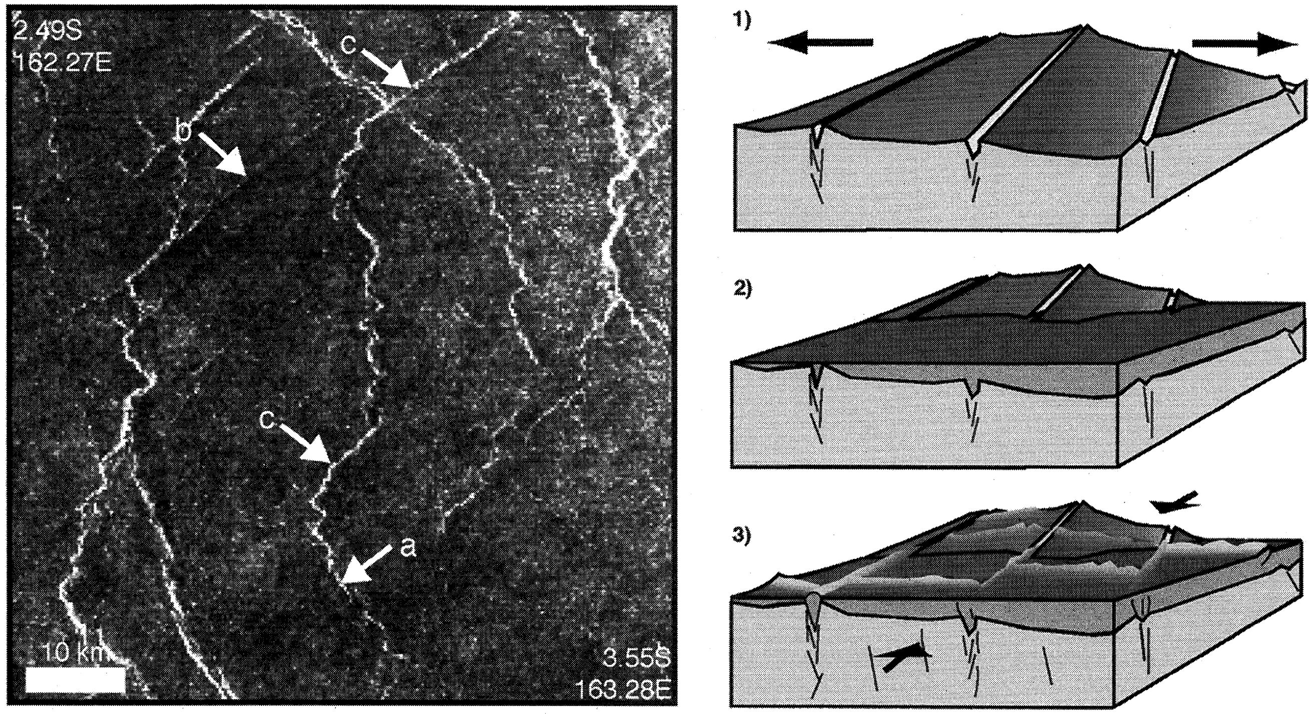

Figure 4. SAR image of orthogonal wrinkle ridges that deform prR2 and a sequence of cartoon block diagrams to illustrate surface evolution. SAR Image from left-look f106S162; dominant wrinkle ridges trend NW (labeled a), consistent with regional patterns. NE trending fractures are filled (labeled b) and structurally inverted due to later contraction, forming NE trending wrinkle ridges (labeled c). Wrinkle ridge interaction with the covered fracture set creates a step-like pattern of NW and NE trending wrinkle ridges. The block diagrams (not to scale) outline the inversion process: (1) prR1 base is cut by NE-trending fractures and uplifted, (2) low-viscosity lava (prR2) flows around resulting topography and fills fractures, and (3) strike-oblique contraction results in wrinkle ridge formation and causes local inversion of fracture fill, creating a step-like pattern of wrinkle ridges in planform.

orientation and characteristics of NE trending wrinkle ridges imply local control by, or reactivation of, the underlying NE trending fracture set. We propose that prR2 lava flows flooded NE trending fractures that cut prR1; after solidification of prR2, strike oblique contraction resulted in structural inversion of the fracture fill creating short, straight NE trending wrinkle ridges. As indicated by current geoid and topography data, contraction is localized in the region of NE trending wrinkle ridges. As the fractures closed because of contractional strain, lava flow fracture fill would have been pushed upward, forming a low linear ridge parallel to and coincident with the earlier formed fracture, in a process similar to terrestrial graben inversion [e.g., *Buchanan and Buchanen,* 1995]. Structural inversion requires the presence of thin flows, filled fractures, and a local contractional environment.

3.1.3. Flood lava flow thickness. In southern Rusalka Planitia, prR2 floods a gentle preexisting topographic basin defined by a warped prR1 surface, as evidenced by the undulating nature of the prR1-prR2 contact, the presence of prR1 kipukas and prR2 outliers, and the spatial correlation of material units with local topographic lows and highs (Plate 1b and Figure 5). This region displays ~0.5 km of topographic relief across ~1 million km^2 (average regional slopes ≤0.002°; Plate 1b). In general, topographic relief across the prR1-prR2 contact is <<0.5 km over 100 km (<<0.3° slope). The shape of the contact, including kipukas of prR1 in prR2 and outliers of prR2 in prR1, taken together with the very gentle topography, indicates an extremely shallow dip (almost flat) of the prR1-prR2 contact. The distribution and character of the NE trending fractures also indicates an extremely shallow dip of the contact between prR1 and prR2. The trace of NE trending fractures in underlying prR1 is discernible in prR2 at distances of 100-300 km from the prR1-prR2 contact (Figures 2 and 4 and Plate 1c), indicating that the prR1-prR2 contact remains relatively flat and shallow across this distance.

These geometric features allow us to constrain the paleodip of the prR1-prR2 contact and therefore estimate the maximum depth (thickness) of prR2 in the map area. Because we currently lack stereo SAR of this region, we cannot determine the detailed topographic character of the fractures, although the available SAR data indicates modest topography. If we assume that at a distance of 100 km from the prR1-prR2 contact the discernable fractures are buried by 10 m of prR2 cover (likely a conservative estimate given that SAR can penetrate ~10 times wavelength in unconsolidated material, in this case giving a depth of ~1 m), the paleodip of the prR1-prR2 contact is ~0.0057° (tan (paleodip) = (prR2 depth)/(distance from contact)). Given this estimated paleodip and ≤400 km distances between exposures of prR1 surrounded by prR2 (Plate 1a), the thickness of prR2 can be conservatively estimated by constructing wedges of prR2 with dips of 0.006°. Following this method, prR2 is estimated as ≤20 m thick across much of the map area. In the northern part of the map area, prR1 is not exposed, although the traces of buried NE trending fractures are

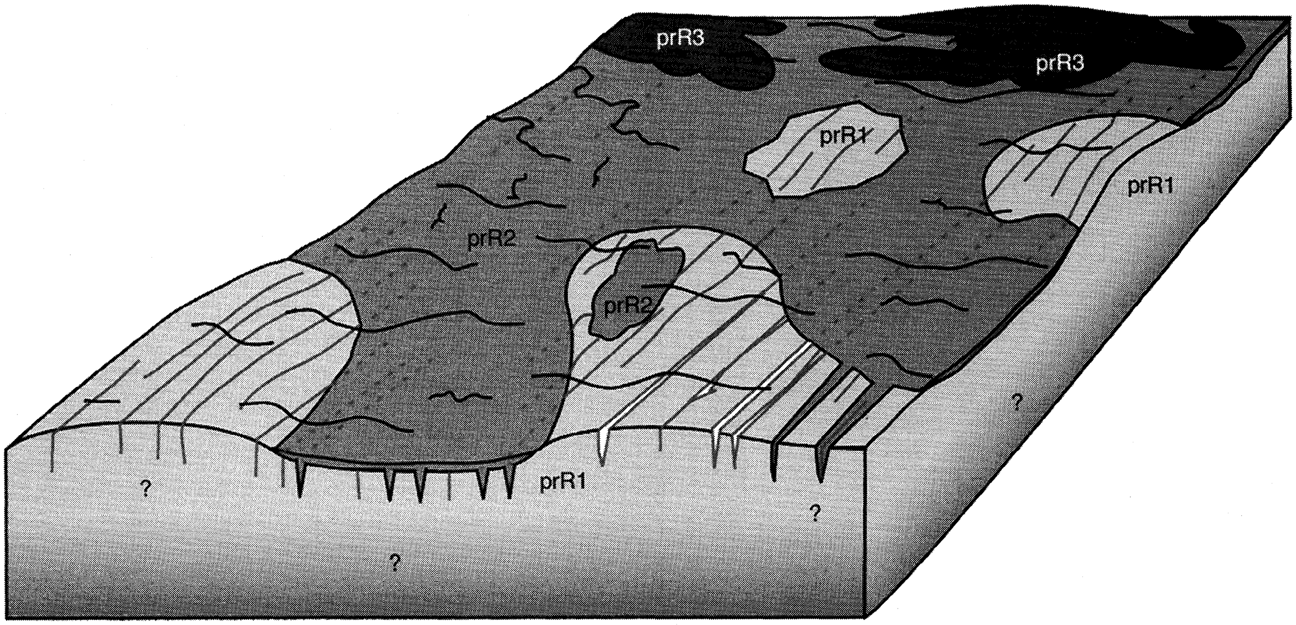

Figure 5. Cartoon block diagram of southern Rusalka Planitia. Note that the vertical scale is highly variably vertically exaggerated; for example, the paleodip of the prR1-prR2 contact is <0.006° (see text for discussion). Low-viscosity flows form the thin, generally coherent prR2. Thicknesses of prR1 and prR3 are unconstrained. Unit prR2 follows early topography and locally fills and truncates extension fractures that cut prR1 (fractures partially covered by prR2 are dotted). Wrinkle ridges cut all three material units and reactivate fractures locally by structural inversion. Note the ratio between depth of fracture and fracture spacing should be ~3:1 following mechanical constraints, but owing to the cartoon nature of Figure 5 the ratio is not illustrated.

discernable in prR2 (Figures 2 and 4a and Plate 1a) indicating that prR2 is quite thin. Because these relations are preserved across the ~9° x 9° region of southern Rusalka Planitia they cannot be dismissed as local marginal details.

The modest thickness of prR2 taken together with the regional distribution of prR2 and the detailed spatial distribution of prR2 and underlying prR1 indicate that prR2 was probably not emplaced from a single point source, but instead prR2 magma probably followed several different pathways to the surface. If prR2 formed as a large sheet flow, we would not expect to see outliers of prR2 unless low-viscosity lava flowed through surface fractures to form outliers. The map relations demonstrated herein could be easily accommodated if prR2 was emplaced to the surface, at least in part, through NE trending fractures. Taken together, the distribution of prR1 and prR2 (kipukas and outliers), the digitate nature of the prR1-prR2 contact, and the character and distribution of NE trending fractures indicate that (1) the composite thickness of prR2 is quite thin, likely < 50 m, (2) prR2 was probably not emplaced from a single point source as one large sheet flow over prR1 based on the presence of kipukas and outliers of both units, and (3) individual flows likely followed different pathways to the surface.

Existing data do not constrain the thickness of prR1 and prR3 (Figure 5). The thickness of prR1 and the possible occurrence of underlying plains units are indeterminable. The spacing of the NE trending fractures does not provide robust mechanical constraints on the layer thickness of prR1. Although the thickness of a fractured layer can be constrained to be ~0.2-0.4 times the spacing of the fractures that cut it [e.g., *Price and Cosgrove*, 1990], we cannot uniquely determine if the fractured layer (and thus fracture spacing) represents part or all of prR1 or a combination of prR1 and older units(s). Such interpretations are simply unconstrained by current data. Unit prR3 is probably quite thin; it lies stratigraphically above prR2, yet it lacks a topographic signature. Therefore, assuming that prR3 does not simply fill a deep hole in prR2, an assumption consistent with the detailed digitate prR2-prR3 boundary and the fact that prR3 forms inliers in prR2, prR3 is likely <<0.5 km thick, the total topographic relief across southern Rusalka plains units. Furthermore, the mottled, radar bright prR3 material forms an irregular contact with prR2, defined by quasi-circular flow patterns around the central peaks of individual shields within prR3, which, together with the lack of topographic relief, is consistent with a thin prR3 layer.

3.2 Geologic History

Crosscutting relations gained from the above relationships allow us to reconstruct the geologic history of southern Rusalka Planitia (Figure 6), and therefore place important constraints on the geological of the processes that affected this region. Nuahine Tessera appears to record the oldest deformation in the region; however, owing to a lack of crosscutting relations we cannot determine the age of the oldest exposed plains (prR1) relative to the tessera host material and its subsequent deformation. There is no evidence that the tessera tectonic fabric exists under the plains east of the Nuahine inlier, as the global stratigraphic model would imply [e.g., *Basilevsky et al.*, 1997]. The parallelism of the tessera folds with the inlier margins is consistent with local (rather than regional) deformation documented at crustal plateaus [e.g., *Hansen et al.*, 1997; *Ghent and Hansen*, 1999]. These rela-

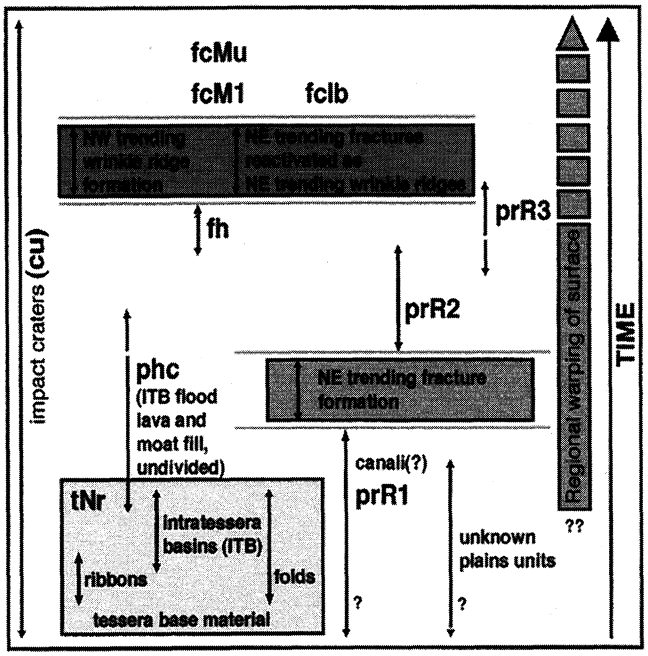

Figure 6. Geologic history of southern Rusalka Planitia.

tions are also consistent with the proposal that tessera inliers represent collapsed and flooded portions of ancient crustal plateaus [e.g., *Phillips and Hansen*, 1994, 1998]. Within the tessera, the material unit deformed by ribbons and folds must predate ribbon-fold tectonism. Because the deformation is likely spatially restricted, the age of the material that hosts this tectonic fabric relative to the age of prR1, the oldest plains unit, is unconstrained. The intratessera basin material of composite phc lacks evidence of tessera-related deformation and thus postdates tessera tectonism. Unit phc embays the local structural topography of the tessera inlier and creates a 20-60 km wide radar dark boundary along the southern and eastern margins of the tessera. This feature is interpreted to be a relict topographic moat, filled by phc flows and later uplifted during regional contraction [*DeShon and Hansen*, 1998]. The composite unit phc may also contain individual flow units related to regional plains lavas. The phc-prR2 contact northeast of Nuahine tessera (outside the study area) is gradational [*DeShon and Hansen*, 1998].

The temporal relationships between prR1 and the Nuahine tessera inlier are unconstrained owing to lack of a coherent contact between the units. In addition, there is no evidence to suggest that tessera terrain underlies prR1 (an assumption of the global stratigraphic model), nor can we use the observed present-day topography of the inlier to constrain the thickness of spatially discrete plains. However, the geologic history of the region after prR1 emplacement is better constrained. NE trending fractures deform prR1 and thus postdate prR1 emplacement. Following and possibly commencing before final prR1 emplacement, broadscale topographic warping began to raise the tessera moat and ridge belt. The preservation of prR1 atop the topographic ridges (Plate 1) indicates that the final increment of ridge formation postdated prR1 emplacement and dominantly predated emplacement of prR2.

The preservation of fractured prR1 kipukas in prR2 and local filling and covering of NE trending fractures by prR2 indicate that prR2 postdates prR1 emplacement and the formation of NE trending fractures. If aging volcanic flows become smoother (and thus become radar darker) with time as a result of progressive weathering [*Arvidson et al.*, 1992], the above sequence is consistent with the observed 1° decrease in RMS slope data. Weathering rates are poorly constrained on Venus, but they are likely to be low [*Wood*, 1997]; therefore the time gap between prR1 and prR2 could be quite large, although it is completely unconstrained by data. Unit phc covers NE trending fractures along its eastern and northern margins, indicating that at least some moat fill flows postdate NE-trending fracture formation and hence emplacement of prR1. The basin west of the class I ridge belt warps prR2 (Plate 1b), implying that broad surface warping continued, at least locally, after prR2 emplacement. The lack of NE trending fractures cutting tessera moat fill suggests that uplift of the moat fill also continued after prR2 emplacement. The cessation of the surface warping is unconstrained.

Shield-sourced prR3 postdates prR2. The prR2-prR3 contact pattern indicates that shield lava flows overlie prR2. If prR2 had flooded preexisting topographically higher shields, we would expect sharp circular contacts, but no such relations are observed.

Wrinkle ridge formation occurred after the emplacement of both prR1 and prR2 and generally after prR3 emplacement. Some prR3 lava flows locally pool along wrinkle ridges, indicating that local prR3 lava flows from individual shields were emplaced synchronous with or after wrinkle ridge formation. However, most wrinkle ridges clearly deform prR3 lava flows; therefore prR3 dominantly predates wrinkle ridge formation. The relative timing between the NW and NE trending wrinkle ridges, resulting from reactivation of flooded NE trending fractures, is unconstrained. However, there is no evidence to suggest that wrinkle ridge suites are diachronous, and the simplest interpretation allowed by the data allows that they are synchronous.

Lava flows from Miralaidji Corona and unnamed corona b (Plate 1a) dominantly postdated wrinkle ridge formation. Local formation of impact craters is assumed to be a globally continuous process, and the age of an individual crater can only be constrained relative to the unit(s) it affects. Alison impact crater (4.0°S,165.6°E) formed on prR1, but temporal relations with the NE trending fractures, prR2, prR3, and wrinkle ridge formation are unconstrained. Similarly, the impact crater Safarmo (10.8°S,161.4°E) postdated phc emplacement, and the unnamed impact crater at 3.1°S,169°E postdated prR2 emplacement.

4. Discussion

Lava flows in southern Rusalka Planitia record a geologic history involving interactions between volcanism, tectonism, and topography. We now evaluate models of plains evolution [e.g., *Basilevsky et al.*, 1997; *Phillips and Hansen*, 1998; *Guest and Stofan,* 1999] in light of the geologic history recorded in southern Rusalka Planitia. Additionally, we evaluate previously proposed lava flow volume and effusion rates.

As a test of the global stratigraphic model, we attempted to correlate the map units identified in this study with published descriptions [*Basilevsky et al.*, 1997; *Basilevsky and Head,* 1998; *Head and Basilevsky*, 1998]. We found that published definitions of the proposed global stratigraphic units proved inadequate to unequivocally identify how the units delineated herein would fit within the global stratigraphic model. The confusion results, at least in part, because material unit descriptions within the global stratigraphic model include tectonic structures, whereas we separate tectonic (i.e., secondary) structures from the material unit they deform. For example, in southern Rusalka Planitia, prR1 is deformed by pervasive wrinkle ridges, thus it correlates to the first order with the Rusalka Group unit "plains with wrinkle ridges" (Pwr_1 and Pwr_2) of *Basilevsky et al.* [1998]. However, the wrinkle ridges of plains with wrinkle ridges [*Basilevsky et al.*, 1997, p. 1057] "are dominantly superposed on primarily undeformed Rusalkian plains...." Yet prR1, which is pervasively cut by NE trending fractures, cannot be described as "primarily undeformed," and therefore prR1 does not correlate with Pwr when described in further detail. Because prR1 hosts fractures, it could also be correlated with either the fractured/ridged plains (Pfr; Lavinia Group) or the densely fractured plains (Pdf; Sigrun Group) of *Basilevsky and Head* [1998]. We cannot fit unit prR1 within the currently published unit definitions of the global stratigraphy model. Problems arise because global stratigraphy unit descriptions imply that tectonic (secondary) structures, such as wrinkle ridges, formed synchronously with material unit emplacement; because tectonic structures are included as unit descriptions, the structures are, by implication, assumed to be primary rather than secondary. Even if wrinkle ridges formed globally synchronously (a statement that cannot be robustly supported by available data), mapping relations in southern Rusalka Planitia indicate that at the type location, wrinkle ridges must postdate emplacement of material unit prR3 (Figure 6).

Unit prR3, a shield-dominated unit, leads to additional questions. Our morphologic description of prR3 based on primary structures most closely matches that of the shield plains unit (Psh) of *Basilevsky and Head* [1998]. *Basilevsky and Head* [1998] place shield plains (Psh) generally as the stratigraphically lowest unit of the Rusalka Group, below plains with wrinkle ridges (Pwr_1 and Pwr_2). However, prR3 postdates prR2, presumably a Pwr unit of *Basilevsky and Head* [1995]. *Basilevsky and Head* [1998] and *Basilevsky et al.* [1997] recognize that locally, Psh materials postdate Pwr_1 and Pwr_2, and therefore our documented stratigraphic relations do not contradict the revised global stratigraphy model. However, placing a material unit both below and above another material unit in a proposed global stratigraphic sequence is self-contradictory. The occurrence of diachronous shield-sourced units is easily explained if each shield-sourced flow comprises spatially and temporally local, not global, units following conclusions based on detailed geologic mapping [e.g., *Guest and Stofan*, 1999; *Addington*, 1999].

Treating volcanic plains emplacement or deformation episodes as widespread globally synchronous events may be juxtaposing sections of geologic time and temporally discrete geologic histories. Determining gross absolute ages for Venus surface evolution requires regions of $\geq$ 20 million km^2 shown to have formed synchronously [e.g., *Phillips et al.*, 1992; *Phillips*, 1993]. Even if such factors can be demonstrated, absolute age constraints are extremely broad and nonunique [e.g., *Campbell*, 1999; *Hauck et al.*, 1998]. The global stratigraphic model fails to allow for potential temporal and spatial overlap of different geological processes. Wrinkle ridge formation, commonly used in the global stratigraphy model as a globally synchronous deformation event [*Basilevsky et al.*, 1997; *Basilevsky and Head*, 1998], has been shown [e.g., *Squyres et al.*, 1992; *McGill*, 1993; *Guest and Stofan*, 1999] to evolve progressively on regional scales. *Guest and Stofan* [1999] outline a similar breakdown of the global stratigraphic model based on coronae-plains relations.

Thickness, volume, and effusion rate estimates presented in the literature are likely significantly overestimated. Previous estimates of plains volumes and effusions rates assumed that Pwr are 1-3 km thick and represent a single flow unit [*Basilevsky et al.*, 1997; *Head and Coffin*, 1997]. However, our analysis indicates that prR2 is likely < 50 m thick. Assuming that prR2 correlates with Pwr of *Basilevsky et al.* [1997], there is no evidence to support the proposed unit thickness of 1-3 km. If prR2 was 1-3 km thick, neither the digitate nature of the prR1-prR2 contact nor details of the filled NE trending fractures in underlying prR1 would be preserved along the prR1-prR2 contact given regional slopes of ≤0.002°. A 1-3 km unit thickness of prR2 would require steep topographic relief (digitate cliffs 1-3 km high) to have existed along the entire prR1-prR2 contact prior to "filling" of this digitate-shaped basin by prR2 flows. Furthermore, prR2 would be required to just fill the digitate basin without any flooding onto the gently dipping prR1 surface. There is no evidence for either the existence of these topographic basins, or for special filling of such basins by prR2. The presence of buried fractures at distances of 100-300 km from the prR1-prR2 contact also indicates that digitate cliffs did not mark the topography prior to prR2 emplacement. In other contributions, *Kreslavsky and Head* [1999] and *Collins et al.* [1999] suggest that minimum paleodips of 0.5° are typical for individual plains units, resulting in unit layer thickness typically >500 m. Given this minimum paleodip, the NE trending fractures that are covered by, but discernable in, prR2 would be buried under 100 m of prR2 at a distance of ~12 km from the prR1-prR2 contact and 500 m of prR2 <60 km from the prR1-prR2 contact. At a distance of 300 km from the prR1-prR2 contact the fractures would be buried under >2.5 km of prR2. It is unlikely that the fractures would be discernable in prR2 if they were covered by even 100 m of prR2. Given that the fractures are discernable at distances of 100-300 km from the prR1-prR2 contact, the paleodip of the contact must be significantly less than 0.5°, and the maximum regional thickness of prR2 significantly less than 500 m. Our analysis indicates a maximum unit layer thickness of at least an order magnitude less than the minimum layer thickness used in unit volume calculations [*Basilevsky and Head*, 1997; *Head and Coffin*, 1997]; therefore volume estimates and dependent magma effusion rates [*Head and Coffin*, 1997] cannot be supported by detailed map relations.

If prR1 and prR2 together comprise Pwr, a "unit" layer thickness estimate is both indeterminate and not relevant to effusion rates. Formation of NE trending fractures clearly occurred temporally between the emplacement of prR1 and prR2 across the map area; therefore, if a composite layer thickness could be determined (because the base of prR1 is not exposed, such a thickness cannot be constrained), it would not be valid to assume that the composite unit (prR1 and prR2) represents a single coherent lava flow or lava flow event. The areal extent of surficial lava multiplied by overestimated thickness produces inflated lava volume values; using these volumes to compute effusion rates compounds the error. Furthermore, absolute time constraints needed to calculate effusion rates are not robust at the spatial or temporal scales required [*Campbell*, 1999; *Hauck et al.*, 1998], especially when considering the possibility of multiple stages of volcanism to produce one coherent unit. Therefore the current plains volume estimates of ~9.2 x 10^8 km^3 and effusion rates from 5 to 7 km^3/yr for Venusian plains [*Head and Coffin*, 1997] are much too high.

Volcanic and structural geologic relations in southern Rusalka Planitia do not allow differentiation between the proposed surface evolution models of *Guest and Stofan* [1999] and *Phillips and Hansen* [1998]. *Guest and Stofan* [1999] proposed a nondirectional volcanic and tectonic evolution of Venus on the basis of a study of over 6 million km^2. They found no evidence for distinct global periods dominated by specific processes such as coronae formation, rift formation, emplacement of flow fields, or shield volcanism. They suggested that these processes repeat over time to form the present-day Venusian surface. *Phillips and Hansen* [1998] proposed that plains volcanism occurred throughout Venus history but that the rate of plains lava emplacement decreased with planet evolution due to lithospheric thickening, the result of mantle cooling. Our focused study on plains formation in southern Rusalka Planitia provides constraints in accord with both models but does not favor one model over the other. To the extent that the models are currently developed, the role of plains evolution in each of these models is similar, and the models, as currently developed, are not themselves mutually exclusionary. Our data indicate that at least one plains unit, prR2, most likely consists of multiple thin flows, compatible with a reoccurring process. In addition, locally consistent NE trending fractures and their interaction with subsequent wrinkle ridge formation reaffirm the importance of local strain patterns and volcanic, topographic and tectonic interactions. Both *Guest and Stofan* [1999] and *Phillips and Hansen* [1998] proposed models in which plains volcanism is a repetitive process that occurs over prolonged periods at local spatial and temporal scales, consistent with the volcanic and tectonic relationships in southern Rusalka Planitia.

In summary, clear delineation and differentiation of geologic material units and tectonic structures in southern Rusalka Planitia results in a detailed geologic history with important implications. (1) Plains unit prR2 is thin (<50 m) across the ~1 million km^2 of southern Rusalka Planitia; there is no evidence for a single point source for the eruption of these flows, and it is possible prR2 flows emerged over widely separated regions along preexisting structures, such as NE trending fractures. (2) NE trending fractures that cut prR1 are filled by prR2 flows and later reactivated during accumulated contractional strain resulting in structural inversion to form local NE trending wrinkle ridges. (3) The geometry of prR1, prR2, and wrinkle ridges with respect to the class I ridge belt provides constraints on tectonic evolution and the emplacement of the plains flow units. The class I ridge belt formation records regional strain for an extended period of time, minimally from the emplacement of prR1 through to wrinkle ridge formation, which broadly postdated emplacement of prR3. (4) Tectonic structures may change appearance over a region yet record the same deformation event, as is the case with the NE trending extension fractures that cut prR1. (5) Topographic evolution and plains volcanism are inextricably intertwined, and the history and geometry of volcanic flow emplacement cannot always be deconvolved.

Southern Rusalka Planitia records the surface expression of a complex volcanic and tectonic local history and the continuing crustal evolution of Venus. Plains formation does not occur as a combination of discrete, unrelated episodes of volcanism and deformation. Rather lava flow emplacement, deformation, and topography form an integrated geologic history recorded in part by the surface. Our mapping supports the proposals that plains evolution is represented by a continuous, locally complex history, rather than discrete, global episodes of plains volcanism [e.g., *Phillips and Hansen,* 1998; *Guest and Stofan,* 1999].

Acknowledgments. This work supported by NASA's Planetary Geology and Geophysics programs under grant NAG5-4609 to Southern Methodist University. Reviews by George McGill and Eric Grosfils were extremely helpful.

References

Addington, E. A., Clusters of small volcanoes on Venus, *Lunar Planet. Sci.* [*CD-ROM*], *XXX,* abstract 1281, 1999.

Anderson, F. S. and S. Smerkar, Implications of atmospheric temperature change for surface deformation on Venus, *Lunar Planet. Sci.* [*CD-ROM*], *XXX,* abstract 1943, 1999.

Arvidson, R. E., R. Greeley, M. C. Malin, R. S. Saunders, N. Izenberg, J. J. Plaut, E. R. Stofan and M. K. Shepard, Surface modification of Venus as inferred from Magellan observations of plains, *J. Geophys. Res., 97,* 13,303-13,318, 1992.

Baker, V. R., G. Komatsu, T. J. Parker, V. C. Gulick, J. S. Kargel, and J. S. Lewis, Channels and valleys on Venus: Preliminary analysis of Magellan data, *J. Geophys. Res., 97,* 13,395-13,420, 1992.

Banerdt, W. B., G. E. McGill, and M. T. Zuber, Plains tectonics on Venus, in *Venus II: Geology, Geophysics, Atmosphere, and Solar Wind Environment,* edited by S. W. Bougher, D. M. Hunten, and R. J. Phillips, pp. 901-930, Univ. of Ariz. Press, Tucson, 1997.

Basilevsky, A. T., On the stratigraphic significance of wrinkle ridges on Venus, *Lunar Planet. Sci., XXVII,* 67-68, 1996.

Basilevsky, A. T., and J. W. Head, Global stratigraphic survey of Venus: Analysis of a random sample of thirty-six test areas, *Earth Moon Planets, 66,* 285-336, 1995.

Basilevsky, A. T., and J. W. Head, Evidence for rapid and widespread emplacement of volcanic plains on Venus: Stratigraphic studies in the Baltis Vallis region, *Geophys. Res. Lett., 23,* 1497-1500, 1996.

Basilevsky, A. T., and J. W. Head, The geologic history of Venus: A stratigraphic view, *J. Geophys. Res., 103,* 8531-8544, 1998.

Basilevsky, A. T., O. V. Nikolaeva, C. M. Weitz, Geology of the Venera 8 landing site region from Magellan data: Morphological and geochemical considerations, *J. Geophys. Res., 97,* 16,315-16,336, 1992.

Basilevsky, A. T., J. W. Head, G. G. Schaber, and R. G. Strom, The resurfacing history of Venus, in *Venus II: Geology, Geophysics, Atmosphere, and Solar Wind Environment,* edited by S. W. Bougher, D. M. Hunten, and R. J. Phillips, pp. 1047-1084, Univ. of Ariz. Press, Tucson, 1997.

Bilotti, F., and J. Suppe, The global distribution of wrinkle ridges on Venus, *Icarus, 139,* 137-157, 1999.

Buchanan, J. G. and P. G. Buchanen, *Basin Inversion*, Geol. Soc., London, 1995.

Campbell, B. A., Surface formation rates and impact crater densities on Venus, *J. Geophys. Res., 104,* 21,951-21,21,955, 1999.

Collins, G. C., J. W. Head, A. T. Basilevsky and M. A. Ivanov, Evidence for rapid regional plains emplacement on Venus from the population of volcanically embayed impact craters,, *J. Geophys. Res., 104,* 24,121-24,139, 1999.

Crumpler, L. S., J. C. Aubele, D. A. Senske, S. T. Keddie, K. P. Magee, and J. W. Head, Volcanoes and centers of volcanism on Venus, in *Venus II: Geology, Geophysics, Atmosphere, and Solar Wind Environment,* edited by S. W. Bougher, D. M. Hunten, and R. J. Phillips, pp. 697-755, Univ. of Ariz. Press, Tucson, 1997.

DeShon, H. R., and V. L. Hansen, Preliminary geologic history of the Diana-Dali Quadrangle (V37), *Lunar Planet. Sci.* [*CD-ROM*], *XXIX,* abstract 1438, 1998.

Farr, T. G., Radar interactions with geologic surfaces, in *Guide to Magellan Image Interpretation,* edited by J. P. Ford, et al., pp. 45-56, Jet Propulsion Lab., Pasadena, Calif., 1993.

Ford, J. P., J. J. Plaut, C. M. Weitz, T. G. Farr, D. A. Senske, E. R.

Stofan, G. Michaels, and T. J. Parker (Eds.), *Guide to Magellan Image Interpretation*, Jet Propulsion Lab., Pasadena, Calif., 1993.

Ford, P. G., and G. H. Pettengill, Venus topography and kilometer-scale slopes, *J. Geophys. Res., 97,* 13,103-13,114, 1992.

Ghent, R. R., and V. L. Hansen, Structural and kinematic analysis of eastern Ovda Regio, Venus: Implications for crustal plateau formation, *Icarus, 139*, 116-136, 1999.

Grimm, R., and P. C. Hess, The crust of Venus, in *Venus II: Geology, Geophysics, Atmosphere, and Solar Wind Environment,* edited by S. W. Bougher, D. M. Hunten, and R. J. Phillips, pp. 1205-1244, Univ. of Ariz. Press, Tucson, 1997.

Guest, J. E., and E. R. Stofan, A new view of the stratigraphic history of Venus, *Icarus, 139,* 55-66, 1999.

Guest, J. E., M. H. Bulmer, J. Aubele, K. Beratan, R. Greeley, J. W. Head, G. Michaels, C. Weitz, and C. Wiles, Small volcanic edifices and volcanism in the plains of Venus, *J. Geophys. Res., 97,* 15,949-15,966, 1992.

Hansen, V. L., J. J. Willis, and W. B. Banerdt, Tectonic overview and synthesis, in *Venus II: Geology, Geophysics, Atmosphere, and Solar Wind Environment,* edited by S. W. Bougher, D. M. Hunten, and R. J. Phillips, pp. 797-844, Univ. of Ariz. Press, Tucson, 1997.

Hansen, V. L., B. K. Banks, and R. R. Ghent, Tessera terrain and crustal plateaus, Venus, *Geology*, *27*, 1071-1074, 1999.

Hauck, S. A., R. J. Phillips, and M. H. Price, Venus: Crater distribution and plains resurfacing models, *J. Geophys. Res.*, *103*, 13,635-13,641, 1998.

Head, J. W., and A. T. Basilevsky, Sequence of tectonic deformation in the history of Venus: Evidence from global stratigraphic relationships, *Geology, 26,* 35-38, 1998.

Head, J. W., and M. F. Coffin, Large igneous provinces: A planetary perspective, in *Large Igneous Provinces: Continental, Oceanic, and Planetary Volcanism, Geophys. Monogr. Ser., vol. 100,* edited by J. J. Mahoney and M. F. Coffin, pp. 411-437, AGU, Washington, D.C., 1997.

Head, J. W., L. S. Crumpler, J. C. Aubele, J. E. Guest and R. S. Saunders, Venus volcanism: Classification of volcanic features and structures, associations and global distribution of Magellan data, *J. Geophys. Res., 97,* 13,153-13,197, 1992.

Herrick, R. R., and R. J. Phillips, Implications of a global survey of Venusian impact craters, *Icarus, 111,* 387-416, 1991.

Ivanov, M. A., and J. W. Head, Tessera terrain on Venus: A summary of the global distribution, characteristics, and relation to surrounding units from Magellan data, *J. Geophys. Res., 101,* 14,861-14,908, 1996.

Kreslavsky, M. A., and J. W. Head, Morphometry of small shield volcanoes on Venus: Implications for the thickness of regional plains, *J. Geophys. Res.*, *104*, 18,925-18,932, 1999.

Kryuchkov, V. P., Ridge belts on the plains of Venus, *Lunar Planet. Sci., XIX,* 649-650, 1988.

Lancaster, M. G., and J. E. Guest, Volcanism and tectonism in Rusalka Planitia and Atla Regio, Venus, *Lunar Planet. Sci., XXV,* 767-768, 1994.

Masursky, H., E. Eliason, P. G. Ford, G. E. McGill, G. H. Pettengill, G. G. Schaber, and G. Schubert, Pioneer Venus radar results: Geology from images and altimetry, *J. Geophys. Res., 85,* 8232-8260, 1980.

McGill, G. E., Wrinkle ridges, stress domains and kinematics of Venusian plains, *Geophys. Res. Lett., 20,* 2407-2410, 1993.

Phillips, R. J., The age spectrum of the Venusian surface, *Eos Trans. AGU, 74(*16*)*, 187, 1993.

Phillips, R. J., and M. A. Bullock, Coupled climate and interior evolution on Venus, *Lunar Planet. Sci.* [*CD-ROM*], *XXX,* abstract 1385, 1999.

Phillips, R. J., and V. L. Hansen, Tectonic and magmatic evolution of Venus, *Annu. Rev. Earth Planet. Sci. 22,* 597-654, 1994.

Phillips, R. J., and V. L. Hansen, Geological evolution of Venus: Rises, plains, plumes, and plateaus, *Science, 279,* 1492-1497, 1998.

Phillips, R. J., R. F. Raubertas, R. E. Arvidson, I. C. Sarkar, R. R. Herrick, N. Izenberg, and R. E. Grimm, Impact crater distribution and the resurfacing history of Venus, *J. Geophys. Res.*, *97,* 15,923-15,948, 1992.

Plaut, J. J., The non-SAR experiments, in *Guide to Magellan Image Interpretation,* edited by J. P. Ford, et al., pp. 45-56, Jet Propulsion Lab., Pasadena, Calif., 1993.

Price, N., and J. Cosgrove, *Analysis of Geological Structures*, 502 pp., Cambridge Univ. Press, New York, 1990.

Rosenblatt, P., P. C. Pinet, and E. Thouvenot, Comparative hypsometric analysis of Earth and Venus, *Geophys. Res. Lett., 21,* 465-468, 1994.

Smrekar, S. E., W. S. Kiefer, and E. R. Stofan, Large volcanic rises on Venus, in *Venus II: Geology, Geophysics, Atmosphere, and Solar Wind Environment,* edited by S. W. Bougher, D. M. Hunten, and R. J. Phillips, pp. 845-878, Univ. of Ariz. Press, Tucson, 1997.

Solomon, S. C., M. A. Bullock, and D. H. Grinspoon, Climate change as a regulator of tectonics on Venus, *Science*, 87-90, 1999.

Squyres, S. W., D. G. Jankowski, M. Simons, S. C. Solomon, B. H. Hager, and G. E. McGill, Plains tectonism on Venus: The deformation belts of Lavinia Planitia, *J. Geophys. Res., 97,* 13,579-13,599, 1992.

Stofan, E. R., V. E. Hamilton, D. M. Janes, and S. E. Smrekar, Coronae on Venus: Morphology and origin, in *Venus II: Geology, Geophysics, Atmosphere, and Solar Wind Environment,* edited by S. W. Bougher, D. M. Hunten, and R. J. Phillips, pp. 901-930, Univ. of Ariz. Press, Tucson, 1997.

Tanaka, K. L., *Venus Geologic Mappers' Handbook, U. S. Geol. Surv. Open File Rep., 94-438,* 50 pp. 1994.

Twiss, R. J., and E. M. Moores, *Structural Geology*, W.H. Freeman, New York, 1992.

Wood, J. A., Rock weathering on the surface of Venus, in *Venus II: Geology, Geophysics, Atmosphere, and Solar Wind Environment,* edited by S. W. Bougher, D. M. Hunten, and R. J. Phillips, pp. 637-666, Univ. of Ariz. Press, Tucson, 1997.

H. R. DeShon, Department of Earth Science, University of California-Santa Cruz, Santa Cruz, CA 95064. (hdeshon@es.ucsc.edu.)

V. L. Hansen, and D. A. Young, Department of Geological Sciences, Southern Methodist University, 2335 Daniel Avenue, Dallas, TX 75275-0395. (vhansen@mail.smu.edu;dyoung@mail.smu.edu.)

(Received August 4, 1999; revised December 7, 1999; accepted December 21, 1999.)